PHYSICAL REVIEW E VOLUME 56, NUMBER 4 OCTOBER 1997

Effects of surface topography on formation of defects in SmC^* devices explained using an alternative chevron description

P. Watson and P. J. Bos
Liquid Crystal Institute, Kent State University, Kent, Ohio 44242

J. Pirs
Jozef-Stefan Institute, University of Ljubljana, Ljubljana, Slovenia

(Received 4 March 1997; revised manuscript received 6 May 1997)

An alternative description of the layer structure of SmC^* devices is used to consider the cause for wide variations in the zigzag defect density in such devices using the same alignment layer material. In this paper, we show how the topography of the surface layer due to imperfect coating techniques and materials promotes the formation of zigzag defects. We show that if the alignment surface slope is greater than the pretilt, high densities of zigzag defects are likely to be present. [S1063-651X(97)50410-7]

PACS number(s): 61.30.−v

I. INTRODUCTION

Due to their highly ordered structure, smectic, and in particular ferroelectric, liquid crystals tend to be very susceptible to defect formation. Since their invention more than 15 years ago [1], much work has concentrated on eliminating zigzag defects from surface-stabilized ferroelectric liquid-crystal (SSFLC) displays. A large amount of this research has focused on determining which alignment materials and surface treatments tend to produce defect-free textures. More recent papers by Koden *et al.* [2], Kanbe *et al.* [3], and others clearly explains the formation of zigzag defects in terms of the pretilt α, the cone angle θ, and the chevron angle δ. Zigzag formation occurs when domains with chevrons pointing in opposite directions are interspersed. The oppositely pointing chevrons have been described in terms of the $C1$ and $C2$ layer structures, with the apex of the $C1$ chevron pointing antiparallel to the rub direction. Geometric necessary conditions for formation of these configurations are as follows:

$$C1 \text{ allowed:} \quad \alpha < \theta + \delta,$$

$$C2 \text{ allowed:} \quad \alpha < \theta - \delta.$$

Thus, by introducing a high pretilt, zigzag defects may be eliminated [4]. Clearly, when the $C2$ condition is met, the $C1$ condition will also hold.

Research relating the cone angle to the chevron angle [5] suggests that, approximately independent of material, $\theta - \delta = 3°$ at room temperature. In other cases, the value may be less than 3°, and may in fact be equal to 0 [6]. Also, as will be discussed below, it is possible that the effective pretilt angle can be negative. This could result from a surface roughness whose magnitude is dependent on the processing conditions of the alignment layer. We would like to consider the possibility that negative values of the effective pretilt could be the cause for high defect densities found in some cases. Unfortunately, the description of the layer structure using the $C1$ and $C2$ definitions is confusing when a negative value of the effective pretilt is allowed.

II. OUR MODEL

Depending on the alignment material and coating technique, angular variations in the surface may be comparable to the pretilt. We may define the angle of variation γ as positive if it tends to make the apparent pretilt angle greater. For a particular surface with angular variations γ ranging from $-\Gamma$ to Γ, with Γ positive, we locally define an effective pretilt $\alpha' = \alpha + \gamma$ (see Fig. 1). To investigate such a configuration, we propose a $C+$, $C-$ layer structure, where the sign refers to the pointing direction of the chevron apex. The $C+$ structure is equivalent to the previously defined $C1$ structure for the case of a high pretilt angle. As shown in Fig. 2, the SmC cones attached to each chevron define the maximum and minimum values of α' from $-(\theta - \delta)$ to $(\theta + \delta)$ can be accommodated by the $C+$ layer structure; and α' from $-(\theta + \delta)$ to $(\theta - \delta)$ can be accommodated by the $C-$ structure. Figure 3 also shows the connections of the definition of the $C+$ and $C-$ layer structures with the $C1$ and $C2$ definitions. The structure defined as $C+$ is seen to be inclusive of a $C1$ structure if α' is positive, but a $C2$ if α' is negative.

As previously pointed out, if α' lies in the range from $(\theta - \delta)$ to $(\theta + \delta)$, then a defect-free structure is expected. Also, if α' is positive [but not necessarily greater than $(\theta - \delta)$], defects may or may not form. A feature that is made clear by this model is that if α' varies from greater than $+(\theta - \delta)$ to less than $-(\theta - \delta)$, then zigzag defects are *required* to form.

III. EXPERIMENT

We used a 1.5% solution of poly (vinyl alcohol) (PVA) in water as the alignment layer for our samples. In order to obtain varied surface topographies, the material was spin-

FIG. 1. Illustration of how effective pretilt may vary from standard pretilt.

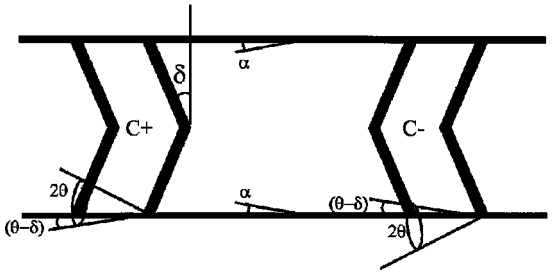

FIG. 2. Definitions of basic chevron structures.

coated onto our substrates at varying speeds. Additionally, we varied the temperature at which the solvent was removed from the substrates. Through the use of these methods, we were successful in obtaining very different surface topography.

Through atomic force microscope (AFM) measurements, we determined that for our spin-coated substrates, there was a radial dependence to the surface properties. By choosing the centers of our cell substrates and our sample for AFM analysis to be equidistant from the spin center, we could ensure that the texture observed in our finished cell was properly correlated to the AFM data.

In constructing our cells, we used 1.5 μm hard-baked photoresist posts for spacers and Merck ZLI-3654 as our liquid crystal, and capillary-filled each cell in the isotropic phase. The center area of each cell was photographed between crossed polarizers. Substrate samples were viewed using a Nanoscope IIIa AFM in the contact mode. A cross section of each substrate surface was analyzed for angular variations, and the rms roughness of the sample was recorded. Thirteen cells with acceptable thickness and uniformity were filled and observed. Using the same mixture of PVA as in the test cells, and using a nematic material with similar $\varepsilon\perp$, we constructed several cells and measured the pretilt using the magnetic null method. We determined the pretilt to be $2 \pm 0.25°$.

IV. RESULTS

In observing the textures of the constructed cells, large variations were apparent between cells and, in some cases, within an individual cell. Some cells had no zigzag defects in the central cell region, some had a small number of defects in this region, while others had very dense, constant arrays of zigzags (Fig. 4). For these large, dense defect structures, generally the defect size was equal to the distance between spacers.

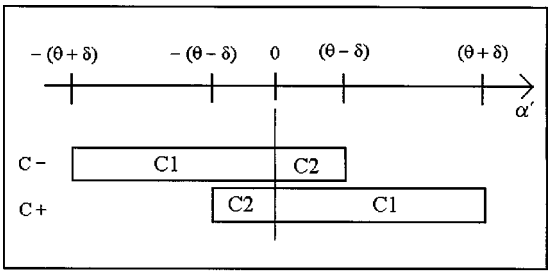

FIG. 3. Allowed chevron structures as a function of effective pretilt. The top rectangle represents the range of α' for $C-$ chevrons, while the bottom rectangle represents the range of α' for $C+$ chevrons.

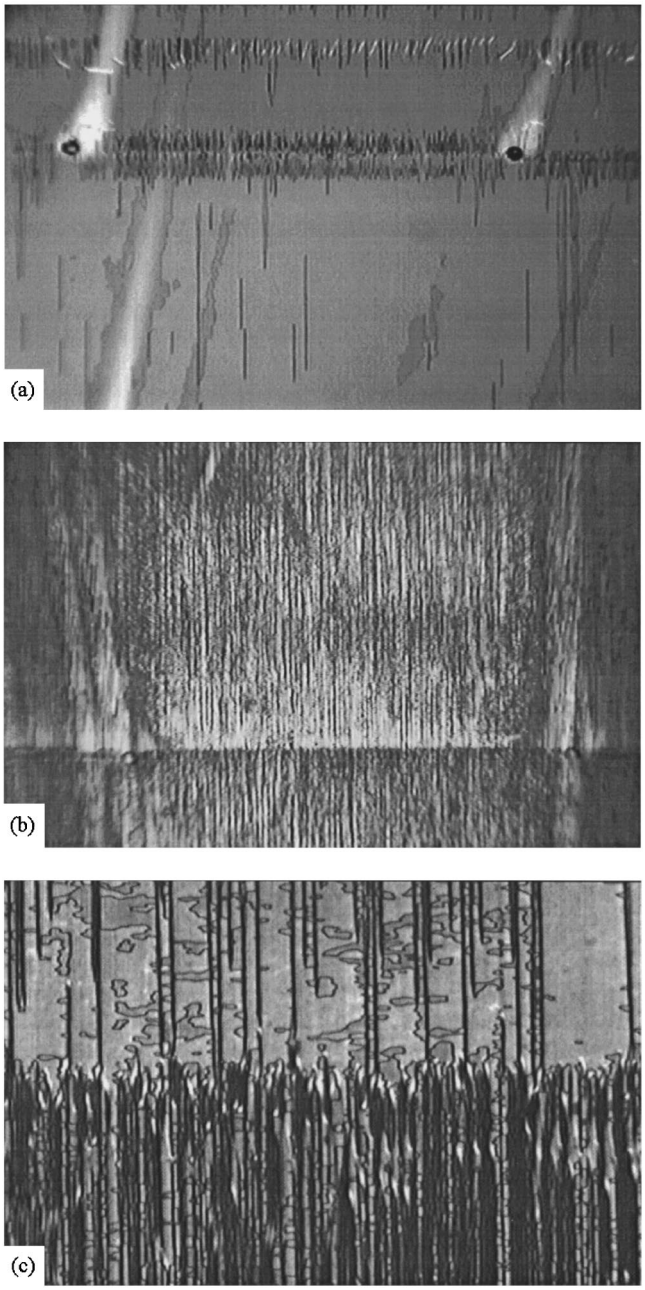

FIG. 4. Defect structure in representative cells. (a) Shows defects in cell 2. The dark circles are spacers, with a separation of 0.25 cm. (b) Shows the defect structure in cell 4. The magnification is the same as in (a). Picture (c) is a detail of (b), magnified 500%.

For a particular cell, to determine Γ, the magnitude of angular variations, a cross-sectional graph of the surface roughness was analyzed. Each point was recorded where the slope change was greater than 0.1° between horizontal distances of minimum size 0.05 μm, and the angle of each connecting segment calculated. In calculating the frequency of occurrence of a particular value of slope, the count was weighted according to the length of each segment. The absolute value of each calculated slope was taken, and this value was placed in bins according to the weight. This histogram was then fitted to a curve (Fig. 5). There was no apparent difference between occurrences of positive and negative slopes. Choosing a cross section parallel or perpendicular to the rub direction also yielded no significant effect.

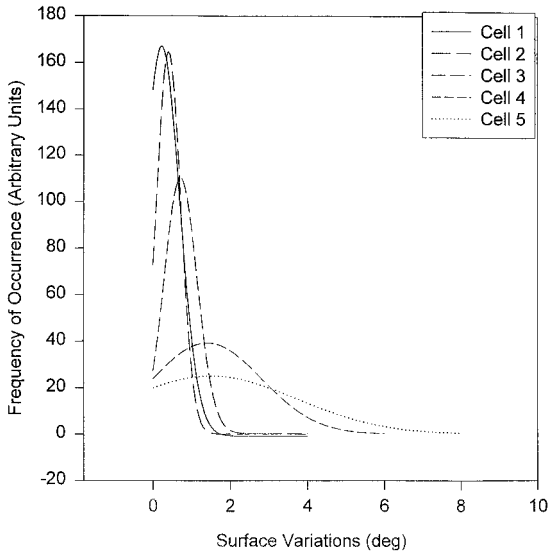

FIG. 5. Histograms of angular surface variations for five representative cells. Bin widths are 0.2° for cells 1, 2, and 3, and 0.6° for cells 4 and 5.

Roughnesses in different samples ranged from ± 0.3 nm to ± 2.2 nm. Maximum angular variation Γ ranged from less than 2° to in some substrates to greater than 4° in others. For the majority of samples, large roughness corresponded to a large angular variation. However, several samples with a very small grain size had a moderately large angular variation despite a low roughness. Both of the cells with very dense defect structures had distances between changes in sign of the surface slope as large as about 200 nm, or approximately 60 smectic layer spacings.

Cells with angular variations of 3.7° and 6.8° had continuous zigzag defects, while for cells with variations of 1.2°, 1.4°, and 1.8° the density of zigzags, which ranged from none to several in the central region of the cell, did not cleanly correspond to the angular variation (Table I). The source of this inconsistency is most likely isolated anomalously high peaks or ridges, which may force the formation of a defect despite the fact that the majority of the surface variations are below the critical angle. We would expect such peaks to form more readily for surfaces with higher roughnesses. Also, a cell with high roughness and low angular variations will be more likely to possess zigzag defects due to its larger grain size, as explained above. Note that the two cells shown in Fig. 5 are the high angular variation cell with the least defects and the low angular variation cell with the most defects. Also interesting is the fact that cell 3 had no apparent zigzag defects. When viewed at higher magnification, this cell demonstrated a woven appearance.

TABLE I. This table shows the relationship between angular variations of the surface and defect densities. The percent of the surface with defects was determined by converting a photograph of the cell into a black and white picture, then comparing the brightness to an area determined to have 100% defects.

Cell number	rms roughness	Maximum angular variation	% of surface with defects
1	0.346 nm	1.4°	16.7
2	0.432	1.2°	25.2
3	0.353	1.8°	0.0
4	1.070	3.7°	64.6
5	2.288	6.8°	75.8

V. CONCLUSIONS

The results show that in cells with angular variations of the surface exceeding the pretilt, the formation of zigzag defects is likely to occur. As a cell is cooled into the SmC^* mesophase, $(\theta-\delta)$ increases from 0 to some final value. Therefore, this work predicts that zigzag defects should form at the SmA-SmC^* transition whenever $\alpha' < 0$ over a sufficiently large horizontal distance. As $(\theta-\delta)$ increases, these defects are no longer geometrically required, and, providing that $\alpha' > -(\theta-\delta)$, they are likely to dissipate.

For angular variations of the surface of magnitude smaller than the pretilt, such defects are less likely to form. However, since the area observed with the AFM is very small compared to the area observed through the microscope, and since a cross-sectional view only looks at a very thin slice of the total surface, it is likely that variations for any sample may be somewhat greater than what is expected from observing the cross section. Any small dust particle or isolated high peak in the surface that exceeds the critical variation angle may cause the creation of a zigzag defect in a seemingly smooth substrate. Thus, in order to guarantee a defect-free low pretilt cell, an alignment surface that is both smooth and uniform is required. This may be achieved through proper choice of materials and well-controlled coating techniques.

ACKNOWLEDGMENTS

I would like to acknowledge the NSF ALCOM (Grant No. 89-20147) for equipment and support. Thanks also to Dr. Oleg Lavrentovich for use of the AFM and Characterization facilities, to Ralph Klouda for technical support and pretilt measurements, and to Dawit Yohannes for AFM training.

[1] N. A. Clark and S. T. Lagerwall, Appl. Phys. Lett. **36**, 899 (1980).

[2] M. Koden, T. Numao, N. Itoh, M. Shiomi, S. Miyoshi, and T. Wada, *Proceedings of the 12th International Display Research Conference, Hiroshima, Japan*, (Society for Information Display, Playa del Rey, CA, 1992), pp. 519–522.

[3] J. Kanbe, H. Inoue, A. Mizutome, Y. Hanyuu, K. Katagiri, and S. Yoshihara, Ferroelectrics **114**, 3 (1991).

[4] Tsuboyama, Y. Hanyu, S. Yoshihara, and J. Kanbe, *Proceedings of the 12th International Display Research Conference*, Ref. [2], pp. 53, 54.

[5] H. Okada, N. Ninomiya, H. Onnagawa, and K. Miyashita, *Society for Information Display International Symposium Digest of Technical Papers* (Society for Information Display, Playa del Rey, CA, 1992), Vol. XXXIII, pp. 239, 240.

[6] H. Okada (private communication).